International Journal of Computational and Experimental Science and ENgineering (IJCESEN)

Vol. 10-No.2 (2024) pp. 112-116
http://www.ijcesen.com

ISSN: 2149-9144

Research Article

Effect of predicted lung mass versus fixed mass regimes on lung dose in SIRT (^{90}Y)

Mohammad ABUQBEITAH[1,2]*, Mustafa DEMİR[1]

[1] Istanbul University-Cerrahpaşa, Cerrahpaşa Medical School, Nuclear Medicine Department, 34098, Istanbul-Turkey
Email: demirm@istanbul.edu.tr - **ORCID:** 0000-0002-9813-1628

[2] Palestine Polytechnic University, School of Medicine, Medical imaging and Nuclear medicine Department, Palestine
* **Corresponding Author: Email:** Qbeta95@hotmail.com - **ORCID:** 0000-0002-3856-3023

Article Info:

DOI: 10.22399/ijcesen.231
Received : 11 March 2024
Accepted : 29 April 2024

Keywords :

^{90}Y dosimetry
Lung mass
Lung dose

Abstract:

This work sought to investigate the impact of fixed lung mass regime versus individualized measures on the lung absorbed dose in ^{90}Y therapy. 14 patients were injected with 3-5 mCi ^{99m}Tc-MAA pursued by whole-body scans with 15% photo-peak window width at 140 keV. SPECT/CT scans were acquired with attenuation and scatter correction. The lung shunt fraction (LSF) was generated from whole-body scans (WBS) and SPECT/CT. Lung volume was measured by contouring the target organ over CT images. Variation, Kruskal Wallis, and Mann-Whitney tests were applied for statistical analysis. In result, 64% of the patients exhibited less than 1 kg lung mass, and the remaining 26% had lung mass larger than 1 kg. The estimated lung shunt fractions from SPECT/CT were greatly lower than planar images with a median of -45% (range: -28 to -69%). The lung dose estimates varied between fixed lung-mass regime used in (TheraSphere Treatment Sheet) and real measures approach with a median difference of 9% and a range from -34% to 76%. However, a significant difference was found in lung dose estimates between planar and SPECT/CT modalities independent of lung mass. It was accordingly inferred that lung mass may vary among patients influencing the predicted dose and the tailored ^{90}Y activity. For precise medicine, the fixed lung mass used on a routine basis should be replaced by patient-specific measures.

1. Introduction

Selective internal yttrium-90 (SIRT-90Y) therapy is a widespread treatment method for unresectable primary and disseminated liver tumors. The unique dual blood supply to the liver paved the way for effective implementation of trans-arterial radioembolization therapy. The hepatocellular carcinoma (HCC) ordinarily receives blood from hepatic arteries, while the portal vein supplies blood to nearly 75% of the healthy liver. Moreover, 80−100% of the hepatic metastases are also fed from the hepatic arteries rather than the portal venous circulation [1]. ^{90}Y is a pure β emitter with a half-life of 64.1 hours that decays into stable zirconium (^{90}Zr) with a maximum and mean energy of 2.3 MeV and 937 keV, respectively. The released beta particles have a maximum penetration of 11 mm and an average of 2.5 mm within soft tissue [2]. In ^{90}Y therapy, the emitted particles are concentrated in microsphere clustering regions.

Unlike other radionuclides (e.g ^{131}I, ^{177}Lu), there is no primary gamma emission except bremsstrahlung radiation emanated from ^{90}Y. Prior to ^{90}Y therapy, visceral angiography is applied to map the blood vessels of tumors and healthy liver components. Afterward, intra-arterial injection of ^{99m}Tc-MAA is applied as a surrogate to ^{90}Y-microsphere [3]. Scintigraphy imaging is subsequently carried out for pulmonary and gastrointestinal shunts assessment and to determine the activity to administer.

The regional beta irradiation is basically to ravage the cancerous cells and spare the healthy injected component. To date, various approaches have been used for dose calculation involving the empirical model, BSA (body surface area) model, MIRD (Medical Internal Radionuclide Dose) formalism, and Partitioning model as well as more recently, voxel-based dosimetry and Monte Carlo simulation

[4,5]. The empirical model has become of rare use due to its primitive and imprecise assumptions. The BSA is a simple and easy to use method assuming that the patient's BSA correlates with the size of the patient's whole liver [6]. In contrast, the partition model (PM) based on MIRD formalism provided patient-specific dose calculations [7].

On the other hand, the dose limits of lung that have been extensively used were defined as 30 Gy in a single treatment and a total of 50 Gy from multiple treatments. Meanwhile, as high as 70 Gy dose limit was reported to healthy injected liver with a small probability of decompensation [8,9]. The lung shunt fraction is classically estimated from planar images obtained after ^{99m}Tc-MAA injection. However, SPECT/CT scan is acquired to explore gastrointestinal shunting and assess tumor uptake. The advent of fused CT images enhanced more accurate liver segmentation, quantification, and volume measurements for the target organs [10].

Herein, the current work explored the effect of using patient-specific lung mass as calculated from CT scans on the lung dose prediction compared to standard 1 kg mass used in daily practice.

2. Material and Methods

Treatment records of randomly selected fourteen patients were reviewed. About 111-185 MBq ^{99m}Tc-MAA was intra-arterially injected into the liver followed by planar imaging and SPECT/CT (Symbia™ T Seri SPECT/CT manufactured by SIEMENS). The photopeak window was set at 140 keV with a 15% width. Subsequently, SPECT/CT scans were acquired encompassing both lungs and liver using the next settings; step and shoot mode, 64 projections/cycle, and 25 seconds /projection. Dual-energy windows DEW (-15%) method was applied for scatter correction. The OSEM-algorithm (10 iterations and 8 subsets) was used for image reconstruction followed by 9-mm low pass filtering.

The LSF from planar imaging was calculated by the below formula [7]:

$$LSF = \frac{\sqrt{Lan \times Lpo}}{(\sqrt{Lan \times Lp} + \sqrt{Liveran \times Liverpo})} \quad (1)$$

Lung anterior count (Lan). lung posterior counts *(Lpo*). liver anterior counts (*Liveran*). and liver posterior counts (*Liverpo*).

Then, the LSFs from SPECT/CT scans were computed by the following equation [7]:

$$LSFspect = \frac{LUNGc}{LUNGc + LIVERc} \quad (2)$$

LSF_{spect}: lungs shunt fraction from SPECT images, $LUNG_c$ + $LIVER_c$ are the summed lung and Liver counts from SPECT slices.

The down-shown equation was utilized to calculate the lung dose [7]:

$$D(Gy) = \frac{A \times 49.3}{M} \quad (3)$$

D: absorbed dose, A: activity (GBq), M: lungs mass (Kg).

The treatment excel-sheet provided by TheraSphere 90Y-glass microsphere considered a fixed lung mass (1 kg) for all patients. However, in this work, the lung doses were estimated using LSFs calculated from planar and SPECT/CT scans based on both fixed lung mass (1 kg) and individualized lung mass for comparison purposes. The lung volume was measured by delineating manual ROIS over CT images with lung window. The lung density was accepted as 0.37 gm/cm^3.

^{90}YDoseCal is an in-house developed 90Y dosimetry code operating with the earlier mentioned functions.

2.1 Statistical Analysis

Non-parametric tests were used as the values showed no normal distribution. First, a significant difference was explored between the groups by Kruskal Wallis Test followed by Mann-Whitney tests.

3. Results and Discussions

The measured volumes and calculated lung masses were summarized in table 1. Accordingly, 64% of the patients exhibited lung mass less than 1 kg, while the remaining 26% had lung mass > 1 kg. The calculated lung shunt fractions from SPECT/CT were smaller than planar images with a median of -45% (range: -28 to -69%), as shown in table 1. Figure 1 illustrates the mean lung dose calculated from different approaches. A variation in the lung doses was manifested according to fixed lung mass (1kg) and patient-specific mass.

Table 1. *Lung volume, mass, and lung shunt fractions (LSFs) for 14 patients.*

Pt	Volume (cm^3)	Mass (kg)	LSF (Planar)	LSF (SPECT/CT)
1	2986	1.10	0.15	0.09
2	1748	0.65	0.03	0.01
3	2510	0.93	0.18	0.11
4	2850	1.05	0.14	0.04
5	4096	1.52	0.07	0.04
6	2503	0.93	0.07	0.03
7	3303	1.22	0.05	0.03
8	3157	1.17	0.13	0.07
9	2035	0.75	0.09	0.06
10	2278	0.84	0.04	0.02
11	1986	0.73	0.06	0.03
12	2469	0.91	0.08	0.05
13	1537	0.57	0.04	0.02
14	1603	0.59	0.07	0.04

The median difference in lung dose estimates between fixed lung mass regime and patient-specific approach was found to be 9% ranging from -34% to 76%. In statistical analysis, the Kruskal Wallis test yielded a significant difference between at least two groups among those illustrated in figure 1. In table 2, Mann-Whitney test results were summarized exhibiting no significant difference between WBS-SM versus WBS-PSM (P_{value} > 0.05), and SPECT/CT-SM versus SPECT/CT-PSM (P_{value} > 0.05). However, a significant difference was found between the other pairs (P_{value} < 0.05). Various types of palliative treatments are implemented in HCC and liver metastases encompassing radiofrequency ablation,

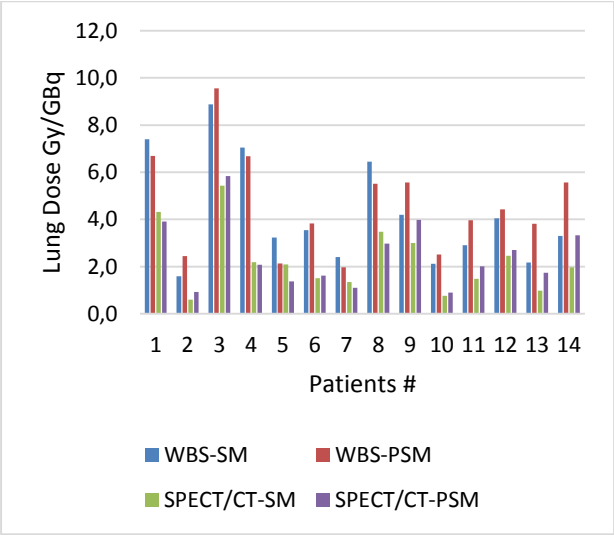

Figure 1. *Lung dose (Gy/GBq) estimates from whole-body scan (WBS) and single photon emission computed tomography/computed tomography (SPECT/CT) based on 1 kg standard lung mass (SM) and measured patient specific mass (PSM).*

Table 2. *Mann-Whitney test results (significant difference at 95%).*

Method Pairs	P_{value}
WBS-SM & WBS-PSM	0.571
WBS-SM & SPECT/CT-SM	0.008
WBS-SM & SPECT/CT-PSM	0.016
WBS-PSM & SPECT/CT-SM	0.001
WBS-PSM & SPECT/CT-PSM	0.004
SPECT/CT-SM & SPECT/CT-PSM	0.734

^{90}Y trans-arterial radioembolization (TARE), and trans-arterial radioembolization (TACE) [10]. Radiofrequency ablation is a first-line treatment for unresectable early-stage patients, while TARE and TACE modalities are commonly followed for inoperable hepatocellular carcinoma. In outcome, several studies reported impressive response and survival benefits after TARE with ^{90}Y microspheres for both primary and metastatic hepatic neoplasms [1,11].

The effectiveness of ^{90}Y therapy is associated with numerical factors, including the injected radioactivity, the target volume, and distribution equivalence between ^{90}Y-microspheres and MAA particles. In this regard, planar and tomographic imaging are substantially used to assess extrahepatic leakages and plan the therapeutic activity. SPECT/CT has been approved superior in quantitative and volume determination with enhanced image contrast [12,13]. In result, a significant difference was found in the lung shunt fractions between standard planar imaging and SPECT/CT with attenuation and scatter correction. In contrast, the mean LSF from SPECT/CT was not significantly different from that estimated by PET/CT after ^{90}Y therapy [14]. So, the LSF values calculated by SPECT/CT scans might be advantageous for those excluded from ^{90}Y therapy due to LSF ≥ 22% calculated from planar imaging. Additionally, the precision in dose estimation may increase the number of therapy sessions controlled by the cumulative lung dose limit, e.g, 50 Gy. The integrated CT images can also be exploited to personalize the lung mass estimation instead of assuming a fixed 1 kg mass in line with the new era of precise medicine. The current evaluation demonstrated that 64% of the patients exhibited lung mass less than 1 kg, and the remaining 26% had lung mass > 1 kg, as calculated from CT scans. Thus, the assumption of standard 1-kg lung mass might clinically underestimate or overestimate lung

dose. For instance, individualized lung mass prediction has been recently reported with a median mass of 839 g (range, 550–1178 g) for men and 731 g (range, 548–869 g) for women by a region-growing tool and a fixed threshold interval of -500 Hounsfield units (HU) at the patient-specific seed point [15]. However, the mean lung volume by ^{99m}Tc-MAA SPECT/CT was slightly smaller than diagnostic CT using the free-breathing technique and Hounsfield units of -734 ± 58 HU [16,17]. In the same context, there was a strong correlation between tumor volume measured on CT and that assessed with surgical specimen [18]. Notably, one-mass-fits-all regime should be replaced by factual patients' specific measures as well as gated ^{99m}Tc-MAA SPECT/CT would provide accurate auto-contouring prediction of the lung.

On the other hand, the widely used partition method and MIRD schema lack the essential compensation of dose heterogeneity over healthy tissues, tumor, and lung. Ideally, Monte Carlo (MC) simulation is the gold standard to compute the energy transport within the tissue and identify non-uniform dose distribution in the target organ. Alternatively, voxel-based dosimetry has been developed as a trade-off method based on dose-point kernels. The dose kernels involve both self-dose and crossfire contribution between the voxels, however, assuming homogenous activity distribution in each voxel is still a drawback [19,20]. Moreover, the range of beta particles is almost voxel-sized making the local energy deposition method feasible to use, however, this feasibility deteriorates in lung dose as the lung density is quite less than soft tissue.

Herein, lung mass measures and LSFs from SPECT/CT with scatter correction have effective impact on the lung dose that propagates to the administered ^{90}Y activity and the number of treatments.

4. Conclusions

It was concluded that the predicted lung dose is highly affected by real lung mass measures in ^{90}Y therapy. A significant difference was found in the dose estimates between the used modalities independent of lung mass.

Author Statements:

- **Ethical approval:** The conducted research is not related to either human or animal use.
- **Conflict of interest:** The authors declare that they have no known competing financial interests or personal relationships that could have appeared to influence the work reported in this paper
- **Acknowledgement:** The authors declare that they have nobody or no-company to acknowledge.
- **Author contributions:** The authors declare that they have equal right on this paper.
- **Funding information:** The authors declare that there is no funding to be acknowledged.
- **Data availability statement:** The data that support the findings of this study are available on request from the corresponding author. The data are not publicly available due to privacy or ethical restrictions.

References

[1]Singh, P., & Anil, G. (2014). Yttrium-90 radioembolization of liver tumors: what do the images tell us?. *Cancer imaging : the official publication of the International Cancer Imaging Society*, *13*(4), 645–657. https://doi.org/10.1102/1470-7330.2013.0057

[2]Roeske, J. C., Aydogan, B., Bardies, M., & Humm, J. L. (2008). Small-scale dosimetry: challenges and future directions. *Seminars in nuclear medicine*, *38*(5), 367–383. https://doi.org/10.1053/j.semnuclmed.2008.05.003

[3]Ilhan, H., Goritschan, A., Paprottka, P., Jakobs, T. F., Fendler, W. P., Todica, A., Bartenstein, P., Hacker, M., & Haug, A. R. (2015). Predictive Value of 99mTc-MAA SPECT for 90Y-Labeled Resin Microsphere Distribution in Radioembolization of Primary and Secondary Hepatic Tumors. *Journal of nuclear medicine : official publication, Society of Nuclear Medicine*, *56*(11), 1654–1660. https://doi.org/10.2967/jnumed.115.162685

[4]Tanyildizi H. (2014). Dosimetric calculations of y-90 microsphere treatment for primary and metastatic liver tumours (dissertation). Istanbul: Istanbul Univ.

[5]Kim, S. P., Cohalan, C., Kopek, N., & Enger, S. A. (2019). A guide to ^{90}Y radioembolization and its dosimetry. *Physica medica : PM : an international journal devoted to the applications of physics to medicine and biology : official journal of the Italian Association of Biomedical Physics (AIFB)*, *68*, 132–145. https://doi.org/10.1016/j.ejmp.2019.09.236

[6]Vauthey, J. N., Abdalla, E. K., Doherty, D. A., Gertsch, P., Fenstermacher, M. J., Loyer, E. M., Lerut, J., Materne, R., Wang, X., Encarnacion, A., Herron, D., Mathey, C., Ferrari, G., Charnsangavej, C., Do, K. A., & Denys, A. (2002). Body surface area and body weight predict total liver volume in Western adults. *Liver transplantation : official publication of the American Association for the Study of Liver Diseases and the International Liver Transplantation Society*, *8*(3), 233–240. https://doi.org/10.1053/jlts.2002.31654

[7]Gulec, S. A., Mesoloras, G., & Stabin, M. (2006). Dosimetric techniques in 90Y-microsphere therapy of liver cancer: The MIRD equations for dose calculations. *Journal of nuclear medicine : official publication, Society of Nuclear Medicine*, *47*(7), 1209–1211.

[8]Walrand, S., Hesse, M., Chiesa, C., Lhommel, R., & Jamar, F. (2014). The low hepatic toxicity per Gray of 90Y glass microspheres is linked to their transport in the arterial tree favoring a nonuniform trapping as observed in posttherapy PET imaging. *Journal of nuclear medicine : official publication, Society of Nuclear Medicine*, *55*(1), 135–140. https://doi.org/10.2967/jnumed.113.126839

[9]Salem, R., Lewandowski, R. J., Gates, V. L., Nutting, C. W., Murthy, R., Rose, S. C., Soulen, M. C., Geschwind, J. F., Kulik, L., Kim, Y. H., Spreafico, C., Maccauro, M., Bester, L., Brown, D. B., Ryu, R. K., Sze, D. Y., Rilling, W. S., Sato, K. T., Sangro, B., Bilbao, J. I., (2011). Research reporting standards for radioembolization of hepatic malignancies. *Journal of vascular and interventional radiology : JVIR*, *22*(3), 265–278. https://doi.org/10.1016/j.jvir.2010.10.029

[10]Giammarile, F., Bodei, L., Chiesa, C., Flux, G., Forrer, F., Kraeber-Bodere, F., Brans, B., Lambert, B., Konijnenberg, M., Borson-Chazot, F., Tennvall, J., Luster, M., & Therapy, Oncology and Dosimetry Committees (2011). EANM procedure guideline for the treatment of liver cancer and liver metastases with intra-arterial radioactive compounds. *European journal of nuclear medicine and molecular imaging*, *38*(7), 1393–1406. https://doi.org/10.1007/s00259-011-1812-2

[11]Bruix, J., Sherman, M., & American Association for the Study of Liver Diseases (2011). Management of hepatocellular carcinoma: an update. *Hepatology (Baltimore, Md.)*, *53*(3), 1020–1022. https://doi.org/10.1002/hep.24199

[12]Garin, E., Rolland, Y., Laffont, S., & Edeline, J. (2016). Clinical impact of (99m)Tc-MAA SPECT/CT-based dosimetry in the radioembolization of liver malignancies with (90)Y-loaded microspheres. *European journal of nuclear medicine and molecular imaging*, *43*(3), 559–575. https://doi.org/10.1007/s00259-015-3157-8

[13]Garin, E., Lenoir, L., Rolland, Y., Laffont, S., Pracht, M., Mesbah, H., Porée, P., Ardisson, V., Bourguet, P., Clement, B., & Boucher, E. (2011). Effectiveness of quantitative MAA SPECT/CT for the definition of vascularized hepatic volume and dosimetric approach: phantom validation and clinical preliminary results in patients with complex hepatic vascularization treated with yttrium-90-labeled microspheres. *Nuclear medicine communications*, *32*(12), 1245–1255. https://doi.org/10.1097/MNM.0b013e32834a716b

[14]Allred, J. D., Niedbala, J., Mikell, J. K., Owen, D., Frey, K. A., & Dewaraja, Y. K. (2018). The value of ^{99m}Tc-MAA SPECT/CT for lung shunt estimation in ^{90}Y radioembolization: a phantom and patient study. *EJNMMI research*, *8*(1), 50. https://doi.org/10.1186/s13550-018-0402-8

[15]Lopez, B., Mahvash, A., Lam, M. G. E. H., & Kappadath, S. C. (2019). Calculation of lung mean dose and quantification of error for ^{90} Y-microsphere radioembolization using ^{99m} Tc-MAA SPECT/CT and diagnostic chest CT. *Medical physics*, *46*(9), 3929–3940. https://doi.org/10.1002/mp.13575

[16]Rosenblum, L. J., Mauceri, R. A., Wellenstein, D. E., Thomas, F. D., Bassano, D. A., Raasch, B. N., Chamberlain, C. C., & Heitzman, E. R. (1980). Density patterns in the normal lung as determined by computed tomography. *Radiology*, *137*(2), 409–416. https://doi.org/10.1148/radiology.137.2.7433674

[17]Kao, Y. H., Magsombol, B. M., Toh, Y., Tay, K. H., Chow, P. K.h, Goh, A. S., & Ng, D. C. (2014). Personalized predictive lung dosimetry by technetium-99m macroaggregated albumin SPECT/CT for yttrium-90 radioembolization. *EJNMMI research*, *4*, 33. https://doi.org/10.1186/s13550-014-0033-7

[18] Pupulim, L. F., Ronot, M., Paradis, V., Chemouny, S., & Vilgrain, V. (2018). Volumetric measurement of hepatic tumors: Accuracy of manual contouring using CT with volumetric pathology as the reference method. *Diagnostic and interventional imaging*, 99(2), 83–89. https://doi.org/10.1016/j.diii.2017.11.002

[19]Maughan, N. M., Garcia-Ramirez, J., Arpidone, M., Swallen, A., Laforest, R., Goddu, S. M., Parikh, P. J., & Zoberi, J. E. (2019). Validation of post-treatment PET-based dosimetry software for hepatic radioembolization of Yttrium-90 microspheres. *Medical physics*, *46*(5), 2394–2402. https://doi.org/10.1002/mp.13444

[20]Santoro, L., Pitalot, L., Trauchessec, D., Mora-Ramirez, E., Kotzki, P. O., Bardiès, M., & Deshayes, E. (2021). Clinical implementation of PLANET® Dose for dosimetric assessment after [^{177}Lu]Lu-DOTA-TATE: comparison with Dosimetry Toolkit® and OLINDA/EXM® V1.0. *EJNMMI research*, *11*(1), 1. https://doi.org/10.1186/s13550-020-00737-8